

INFRARED-SELECTED “WARM” GALAXIES OBSERVED IN X-RAYS

PAUL J. GREEN, MARTIN WARD, SCOTT F. ANDERSON, AND BRUCE MARGON

Astronomy Department and Physics Department, University of Washington

M. H. K. DE GRIJP

Sterrewacht Leiden

AND

GEORGE K. MILEY

Space Telescope Science Institute

Received 1988 February 11; accepted 1988 September 1

ABSTRACT

Infrared, optical, and X-ray observations are presented for a sample of “warm” infrared selected galaxies listed in the IRAS Point Source Catalog. These galaxies have also been observed serendipitously in X-rays by the *Einstein Observatory*. From low-resolution optical spectra, we find that all have emission lines, indicating a Seyfert or H II region type nucleus. Many of these galaxies were previously uncataloged. Based on the X-ray detection rate of our small sample, we conclude that large numbers of warm *IRAS* Seyfert 1–1.9 galaxies may be detectable in X-rays by future surveys such as ROSAT.

Subject headings: galaxies: Seyfert — infrared: sources — X-rays: sources

I. INTRODUCTION

Active galactic nuclei (AGNs), particularly quasars and Seyfert 1 galaxies, are often found to be strong X-ray emitters. A signature of powerful nuclear activity in galaxies, strong emission lines, are a characteristic of these and of somewhat less luminous classes of active galaxy, e.g., Seyfert 2 galaxies and galaxies that are not Seyfert galaxies, but contain gas in their nuclei photoionized by OB stars. Non-Seyfert galaxies with emission lines characteristic of H II regions are often called “starburst” galaxies (e.g., Balzano 1983). In addition to the quasars and Seyfert 1 galaxies, many Seyfert 2 and starburst galaxies have been detected in X-rays by the *Einstein Observatory* (Kriss, Canizares, and Ricker 1980; Fabbiano, Feigelson, and Zamorani 1982).

Seyfert galaxies have been discovered through a variety of means, each with its own intrinsic selection biases. The Markarian ultraviolet (UV) excess survey is, with a few exceptions, insensitive to AGNs which are heavily reddened or contaminated by starlight. Radio surveys of AGNs may suffer from a different bias: for a given optical luminosity, radio bright quasars are 3 times as luminous in X-rays as their radio quiet counterparts (Tananbaum *et al.* 1983), but only ~10% of quasars are radio loud. Other, lower luminosity radio-selected AGNs might also suffer from similar, hidden X-ray biases.

Seyferts can also be selected via their 25 μ m and 60 μ m infrared characteristics. The *Infrared Astronomical Satellite* (*IRAS*) has detected many galaxies in the mid-infrared (Soifer *et al.* 1984; Young *et al.* 1984), most of which have fairly steep infrared spectra. Many quasars and active galaxies exhibit a significantly flatter spectrum in the infrared. Several studies, for example, De Grijp *et al.* (1985) used this characteristic to select a subsample of “warm” objects from the *IRAS* Point Source Catalog (1985, hereafter PSC). After removal of galactic objects, more than 70% of the remaining galaxies are Seyferts, quasars, or low-ionization nuclear emission-line regions (LINERS; Heckman 1980), and another 20% are H II region galaxies or starbursts. This technique has revealed a large number of previously uncataloged AGNs. A small number of

these have been observed in hard X-rays by *EXOSAT* (Ward *et al.* 1988).

Here we report results of a study which adopts slightly modified infrared selection criteria, together with the requirement that the object be observed in soft X-rays by the *Einstein Observatory* and not coincide with a bright star on the Palomar Observatory Sky Survey (POSS). Not only is this method complementary to UV, radio, or X-ray samples, but it permits study of correlations between the infrared and X-rays in a sample with well-defined characteristics in these bands. A more detailed discussion of these correlations, as well as comparisons of the properties of our infrared-selected galaxies with characteristics of other samples of active galaxies, will be presented in a forthcoming paper. In the present work, we report the new X-ray detections and upper limits, and comment on their significance to future X-ray observations of “warm” *IRAS*-selected galaxies.

II. OBSERVATIONS AND SELECTION CRITERIA

a) Infrared Observations

The PSC, which covers more than 96% of the sky at wavelengths of 12, 25, 60, and 100 μ m, contains some 250,000 sources (Neugebauer *et al.* 1984). Some 20,000 galaxies are detected, usually at 60 or 100 μ m, and ~50% appear in existing catalogs. From the PSC, we culled objects at high galactic latitude ($|b| \geq 20^\circ$) which are not in the directions of the LMC or the SMC. To examine only “warm” galaxies, we adopt selection criteria similar to De Grijp, Miley, and Lub (1987) and Kailey and Lebofsky (1988). We require that the spectral index α between 25 and 60 μ m (defined by $f_\nu \propto \nu^\alpha$, where f_ν is the flux density at frequency ν), be greater (flatter) than -1.5 in the PSC version 1. This corresponds to a flux density ratio $f_{25}/f_{60} \geq 0.269$. Because some of the fluxes have been revised in the PSC version 2.0 and in co-added scans, this criterion, if applied to these later data sets, would inevitably yield a somewhat different sample. In addition, we select only galaxies detected at 25 μ m with an *IRAS* flux quality flag of 2 or better. This helps eliminate spurious objects while removing the

requirement of a detection at $60\ \mu\text{m}$, where a low enough upper limit still insures that the spectral slope is "warm."

b) X-ray Observations

The *Einstein Observatory* Imaging Proportional Counter (IPC) and High-Resolution Imager (HRI) fields, covering some 4% of the sky, were searched for positional overlap with the warm objects selected from the PSC. Positional uncertainties in the IPC and in the PSC are both $\approx 1'$, so we require the X-ray and *IRAS* positions to be within $90''$ for the object to be called an X-ray detection. In the final list presented here, it happens that only IPC-observed objects satisfied all our criteria. In order to avoid complicating the selection bias of our sample, we reject any objects that were the intended targets of the X-ray fields, since these are presumably weighted toward UV-excess, radio, or optically selected galaxies.

Our criteria for calling an *IRAS* "warm" galaxy a detection in the IPC, described briefly here, are adopted from Anderson and Margon (1987). The standard IPC reprocessing (Harnden et al. 1984) includes two automated source searching algorithms, one useful for finding isolated point sources, the other better at finding sources that are extended or in confused regions. We also performed a third test for source existence using a circular detection window of radius $3'$ centered on the position of the galaxy. A background is estimated from the intensity in a concentric annulus extending from $3'$ to $5'$ radius whenever possible, excluding nearby sources from the annulus if necessary. Counts corresponding to pulse height channels from the 0.5–3.0 keV energy range are used. Flux estimates are made by assuming a canonical X-ray spectral energy index α_x of -0.7 (Petre et al. 1984), and we include corrections for absorption by neutral hydrogen as a function of position in our galaxy using the values of column density, N_H , given by Heiles (1975) or by Marshall and Clark (1984). Tananbaum et al. (1979) have shown that the mean uncertainty in broad-band fluxes resulting from a combined effect of varying α_x from 0 to -1 and N_H from 0 to $10^{21}\ \text{cm}^{-2}$ is only $\pm 15\%$.

The methods described above can fail to find genuine sources in confused regions, or in the neighborhood of a strong X-ray source, due to contamination of the local background. For these cases, we have made X-ray contour maps from the IPC data of $17' \times 17'$ squares including the galaxy of interest. The data are convolved with a two-dimensional gaussian of FWHM $64''$, and a background estimation from a large area is performed to better average over small-scale fluctuations in the neighborhood of the galaxy.

Assuming Poisson statistics, a given source is accepted as an X-ray detection only if it satisfies two or more of the following criteria (Anderson and Margon 1987): (1) $\geq 5\ \sigma$ detection in the automatic source-finding algorithms; (2) $\geq 2.6\ \sigma$ detection in our third, independent technique; (3) $\geq 3\ \sigma$ detection in a smoothed contour map.

c) Optical Observations

Visual examination of the POSS suffices to eliminate bright galactic objects which otherwise satisfy our criteria. The majority of the objects remaining are galaxies, clearly extended on the POSS, with apparent magnitudes $B \lesssim 16$. Galaxies much fainter than this are not likely to be detected by *IRAS*. In this paper, we discuss only objects for which we have both X-ray information and optical redshifts.

Considering only those candidate objects which are obviously galaxies, or at least stellar in appearance while lacking

diffraction spikes, we have optical spectra for 16 out of 26. Because the majority of those lacking optical data (seven out of nine) are uncataloged, it is unclear how many objects in this group will turn out to be galaxies. Given the stated selection criteria, we can say that the extragalactic sample is more than 62% complete. Limitations in right ascension and declination, and not any intrinsic optical selection effect, are responsible for this incompleteness.

We have obtained low-resolution optical spectra for these objects using the 3.6 m ESO telescope at La Silla, and the 2.5 m Isaac Newton telescope at La Palma (De Grijs, Miley, and Lub 1989). Details of the observations are given in Table 1. The fluxes, centers and equivalent widths of emission lines were measured, and objects with stellar spectra that had not been identified as stars from the POSS were eliminated. Continuum fluxes at $4400\ \text{\AA}$ were also measured, and redshifts were determined from the average of several of the stronger emission lines.

III. DATA

In Table 1 we list the observed fluxes for all our sample galaxies for which we have redshifts. These objects satisfied the selection criteria using the first version of the PSC, but the $25\ \mu\text{m}$ flux densities quoted are taken from the revised version (2.0). In this new version, some fluxes less than 2 Jy have been corrected for a flux overestimation problem near the catalog threshold sensitivity. In most cases, however, the fluxes are revised by only a few percent. The X-ray fluxes listed in Table 1 are derived using a background calculated from a circular annulus around the source, as described above (§ IIb). We list optical emission-line fluxes and, when available, continuum flux densities at $4400\ \text{\AA}$ and photographic magnitudes cataloged by Zwicky et al. (1961).

For the optical photometry, we obtain the integrated flux density (f_b in $\text{ergs cm}^{-2}\ \text{s}^{-1}\ \text{\AA}^{-1}$) using $\log f_b = -0.4 m_b - 8.17$ (Allen 1973). The blue magnitude m_b is found using photographic magnitudes from Zwicky et al. (1961) and $m_b = m_{pg} + 0.11$. The flux density at $4400\ \text{\AA}$ (f_{4400} , same units as above) is measured from the narrow slit spectra. The flux is taken to be the product of wavelength and flux density. The ratio of integrated flux to spectroscopic, small-aperture blue flux is presented in Table 2 as L_b/L_{4400} when both values are available. This provides some indication of the dominance of the nuclear emission; those with low ratios have a strong nuclear component. Optical measurements have not been corrected for reddening.

Table 2 contains the redshifts and luminosities for our sample. The luminosities are calculated assuming $H_0 = 50\ \text{km s}^{-1}$ and $q_0 = 0$. An exception to this is *IRAS* 12232+1256 (NGC 4388) in the Virgo cluster, for which we use the weighted mean distance modulus of 31.32 calculated by Rowan-Robinson (1985), yielding a distance of 18.4 Mpc. Table 2 also includes the values of N_H used to calculate L_x .

IV. INDIVIDUAL OBJECTS

We shall briefly discuss each X-ray identified galaxy in order of right ascension. Figure 1 shows narrow slit optical spectra for four selected objects.

IRAS 02071–1023.—This galaxy, also selected by the Markarian survey, is Mrk 1022 (NGC 838). We did not obtain an optical spectrum, but fortunately it is included in a survey by Keel et al. (1985). They classify it as an H II region galaxy. There are three other optically bright galaxies and four X-ray

TABLE 1
OBSERVED CONTINUUM AND EMISSION-LINE FLUXES FOR X-RAY OBSERVED IRAS WARM GALAXIES

Name	Spectral Mode ^a	X-Rays ^b	25 μ m (Jy)	m_b ^c	4400 Å ^d	(H α + [N II]) ^e	[O III] ^{e,f}	H β ^e
00344–3349 (ESO 350–IG 38)	A	<23.4	2.520	14.5	47.8	143.9	133.2	27.7
01356–1307	A	<31.1	0.472	...	11.0	16.9	22.7	0.5
01475+3554	B	<17.5	0.317	...	3.9	4.71	3.3	0.4
02071–1023 ^g (Mrk 1022)	D	26.7	1.83	12.5	...	62.5	3.23	6.7
02072–1025 (NGC 839)	B	<13.9	1.99	12.5	4.7	4.0	0.52	<0.3
04124–0803 ^h	A	220	0.541	15.7	32.7	71.0	82.9	6.0
04596–2257	A	69.0	0.264	...	28.1	23.5	6.1	4.3
10282+2903 (NGC 3265)	C	<8.0	0.670	14.1	13.0	14.4	1.2	1.36
12232+1256 (NGC 4388)	A	50.3	3.55	12.3	7.4	44.3	76.8	5.2
12543–3006	A	<116.4 ⁱ	0.462	...	3.9	4.8	4.0	<0.4
14070+2636 (HARO 40)	B	<48.1	0.230	15.8	2.5	8.7	4.3	2.4
14434+2714	C	9.8	0.341	15.5	4.3	5.0	5.3	0.5
15217+0843	C	<20.9	0.340	15.7	3.8	5.0	28.5	<0.1
17296+5940	C	<17.0	0.090	15.5	1.5	2.2	1.2	<0.2
20450+0013	B	<12.0	0.420	14.4	10.0	2.6	2.5	<0.4
23461+0157	A	<31.0	0.635	15.4	6.6	14.3	0.6	0.8

NOTE.—A colon denotes an uncertain measurement.

^a Spectral Modes: telescope; aperture and resolution (FWHM): (A) La Silla ESO 3.6 m; 4" \times 4", 11 Å. (B) La Palma INT 2.5 m; 4 Å. Narrow slits used range from 1" to 1".5. (C) La Palma INT 2.5 m; 8 Å. Narrow slits used range from 1" to 1".5. (D) Mount Lemmon UM/UCSD 1.5 m; 4" (diameter), 15 Å.

^b (0.5–3.0 keV, 10^{-14} ergs cm⁻² s⁻¹). X-ray upper limits are 2.6 σ except as noted for IRAS 14070, 12543, and 23461.

^c Photographic magnitudes from Zwicky *et al.* (1961) have been converted to m_b (see § III). An exception is noted in footnote ^g. Directly observed blue magnitudes are listed for IRAS 00344 (Veron-Cetty and Veron 1987).

^d From spectra; 10^{-16} ergs cm⁻² s⁻¹ Å⁻¹.

^e 10^{-14} ergs cm⁻² s⁻¹.

^f Sum of 5007 Å and 4959 Å lines.

^g Optical data from Keel *et al.* 1985.

^h X-ray data from Steiner, Grindlay, and Maccacaro 1982.

ⁱ X-ray emission dominated by cluster.

TABLE 2
REDSHIFTS AND LUMINOSITIES

Name	Type	z	N_H ^a (10^{20} atoms cm ⁻²)	$\log L_x$ (0.5–4.5 keV)	$\log L_{25}^b$	$\log L_b^c$	$\log L_{4400}$	(L_b/L_{4400})
00344–3349	H II	0.020	2.80	<41.76	44.72	43.92	43.56	2.3
01356–1307	S2	0.040	2.20	<42.48	44.59	...	43.52	...
01475+3554	S2	0.080	6.10	<42.85	45.02	...	43.67	...
02071–1023	H II	0.013	2.78	41.41	44.20	44.34
02072–1025	H II	0.013	2.80	<41.14	44.24	44.34	42.18	145.
04124–0803 ^d	S1	0.038	...	43.14	44.63	43.99	43.95	1.1
04596–2257	NL S1	0.041	2.79	42.81	44.36	...	43.93	...
10282+2903	H II ^e	0.004	2.80	<40.30	42.74	42.67	41.60	11.7
12232+1256	S2	0.008	3.92	40.46	43.23	43.16	41.16	100.
12543–3006	S2	0.055	6.13	<43.34	44.86	...	43.35	...
14070+2636	H II	0.060	3.30	<42.81	44.63	44.34	43.47	7.4
14434+2714	S1.9	0.029	3.35	41.70	44.17	43.83	43.81	1.0
15217+0843	H II	0.037	2.23	<42.23	44.38	43.96	43.00	9.1
17296+5940	S2	0.028	5.02	<41.91	43.56	43.80	42.36	27.5
20450+0013	H II	0.012	8.36	<41.07	43.50	43.51	42.43	12.0
23461+0157	S2	0.031	6.13	<42.27	44.50	43.93	43.08	7.8

NOTE.— L_{25} , L_b , and L_{4400} calculated in observed frame.

^a From Heiles 1975 or Marshall and Clark 1984.

^b The 25 μ m luminosity L_{25} is calculated from flux $F_{25} = v_{25} f_{25}$, where v_{25} is the rest frequency of 25 μ m and f_{25} is the 25 μ m flux density observed by IRAS.

^c L_b calculated from photographic magnitudes given by Zwicky *et al.* 1961 (see § III).

^d X-ray data from Steiner, Grindlay, and Maccacaro 1982.

^e Classification difficult due to poor signal-to-noise in optical spectrum.

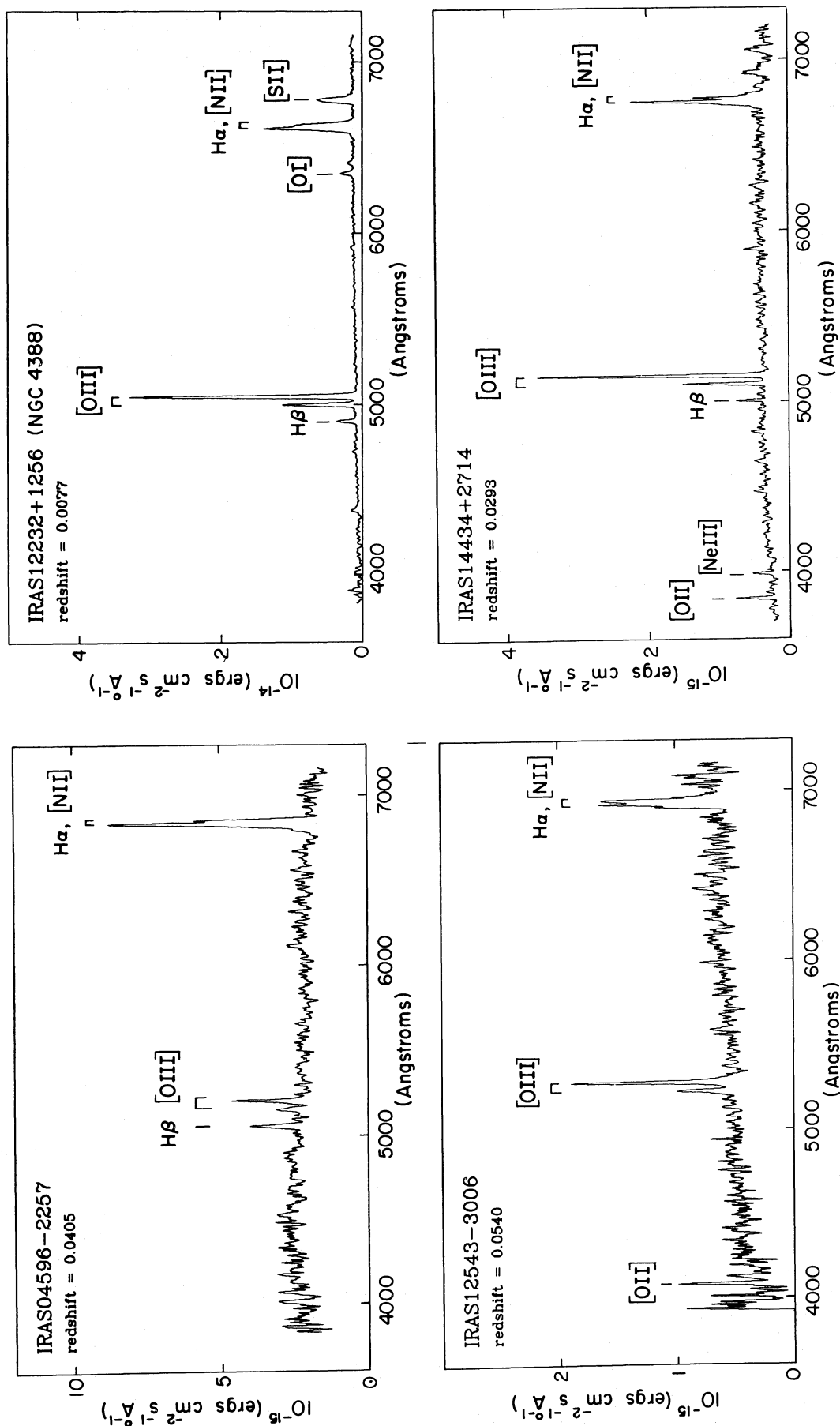


FIG. 1.—Optical spectra of four “warm” IRAS galaxies. All are detected in X-rays except IRAS 12543. The latter is in a region of extended cluster X-ray emission.

sources greater than or equal to 4σ above background in this very interesting IPC field. One of these is not coincident with any obvious optical counterpart, one is identified with a star, and another is close to the pair NGC 833/NGC 835 = Mrk 1021. IRAS 02072 (NGC 839), in the same field, is a flat-spectrum IRAS galaxy with only an X-ray upper limit. This field is also a source of hard X-rays detected by the *HEAO 1* A-1 satellite (Wood *et al.* 1984). We do not know at this stage which of the soft X-ray sources might also be responsible for the hard (2–10 keV) X-rays. It is possible that the hard X-ray source is confused, but more probably, one of these AGNs is a Seyfert 1 and therefore the likely counterpart of the hard X-ray source.

IRAS 04124–0803.—This Seyfert 1 was discovered serendipitously in X-rays by Steiner, Grindlay, and Maccacaro (1982). Based on the data they present, this galaxy easily fulfills our criteria as an X-ray detection. The optical spectrum shows broad Balmer lines, with an integrated ratio of $H\alpha/H\beta$ of 9.2. This is steeper than average for Seyfert 1 galaxies and may indicate some internal reddening, but the blue *UBV* colors preclude a high continuum reddening.

IRAS 04596–2257.—The spectrum of this galaxy (see Fig. 1) appears to be an example of a Seyfert 1 with unusually narrow permitted lines for the class. The $H\beta$ emission line has a FWHM velocity significantly larger than [O III], arguing against classification as an H II galaxy. In addition, it is clear that the $H\alpha$ emission line has broad wings beyond the profile expected from blending with [N II] $\lambda\lambda 6548, 6584$. Further evidence that this galaxy is not a Seyfert 2 is based on the ratio of [O III]/ $H\beta$, which is too low for a nucleus of that class.

Although the FWHM of $H\beta$ is less than 1500 km s^{-1} , the best estimate from the present data is that this is a narrow-line Seyfert 1 galaxy, of the type discussed by Osterbrock and Pogge (1985). Our suggestion is consistent with the observed X-ray luminosity, which would be anomalously high if the galaxy were either an H II galaxy or a Seyfert 2 galaxy. Higher resolution spectral data are clearly needed in order to confirm its Seyfert 1 nature.

IRAS 12232+1256.—This galaxy is also known as NGC 4388, a previously studied edge-on Seyfert 2 for which Phillips and Malin (1982) measure an intrinsic absorption $A_v = 1.5$. Its spectrum appears in Figure 1. The large ratio L_b/L_{4400} of large to small aperture blue luminosity (Table 2) is a result of the size and proximity of this galaxy compared with others in our sample. The X-ray luminosity is somewhat weak relative to other Seyfert 2 galaxies. This may be due in part to absorption of the soft X-rays by material intrinsic to the galaxy.

NGC 4388 was included in the survey of disk galaxies by Stauffer (1982). We note that his measured [O III] flux is within 15% of our value. NGC 4388 was also observed by Filippenko and Sargent (1985), who claim to detect faint broad wings to the $H\alpha$ line. If correct, NGC 4388 would become by far the least X-ray luminous Seyfert 1 galaxy so far detected.

IRAS 12543–3006.—The target of the *Einstein* observation was the southern cluster Klemola 22. The warm IRAS galaxy lies a few arc minutes west of the central region of this cluster, but without a spectroscopic redshift for the cluster galaxies, we cannot be certain that IRAS 12543 is a cluster member. This question is of interest because of its broad, strong [O III] emission lines (see Fig. 1). The X-ray contours extend over $\sim 7'$, and it appears likely that IRAS 12543 is a point source blended with the diffuse X-ray emission (see Fig. 2). There are other X-ray enhancements that may be due to unresolved X-ray

emission from cluster members. Because of both the extended X-ray emission, and the doubt concerning its cluster membership, we list X-ray information for IRAS 12543 as upper limits.

IRAS 14434+2714.—This galaxy is a face-on spiral. The spectral classification is ambiguous based on the present data. A Seyfert 2 would seem to be the appropriate class except for the fact that close inspection of the $H\alpha$ line reveals broad wings at the base (up to 4000 km s^{-1} at full width zero intensity), whereas the $H\beta$ line lacks detectable wings (see Fig. 1). This evidence would then imply that the galaxy is a Seyfert 1.9. The ratio of wide to narrow slit blue luminosity, nearly unity, is consistent with the predominant nuclear emission expected from a Seyfert 1 as compared to a starburst or H II region galaxy.

It is important to recognize the distinction between objects such as this, and for example IRAS 04596 discussed above. In the case of Seyfert 1.9 galaxies, the broad-line region (BLR) is evident with velocity width typical of Seyfert 1 galaxies, but due to heavy obscuration its observed strength is weak and may not be detected at all in the $H\beta$ line. In the case of narrow-line Seyfert 1 galaxies like IRAS 04596, the nucleus may not be significantly reddened; the permitted line profiles simply have an intrinsically low velocity width. Both cases can prove difficult to recognize, and lead to misclassification as Seyfert 2 galaxies. The distinction is important since by definition Seyfert 2s have no detectable BLR. Whether in fact *all* Seyfert 2 galaxies have a BLR not observable directly along a line of sight to the nucleus is beyond the scope of this discussion. For practical reasons it is useful to distinguish between nuclei with directly observable broad-line gas, and those without.

Two of the galaxies in this sample, IRAS 14070 and 23461, merit some further discussion of their X-ray observations. Both are starburst galaxies and both are placed, by unfortunate coincidence, near enough to X-ray bright objects that our conservative X-ray detection criteria were not satisfied.

IRAS 14070 proved to be a detection in X-rays at $\sim 4\sigma$ or greater when we subtracted a local background with algorithms described above, excluding a nearby quasar (PG 1407+265) from the background annulus. The galaxy was not detected via the automated algorithms, and so to satisfy our criteria must be a detection of 3σ or greater on a smoothed contour map. We did find a $\approx 3\sigma$ contour $\approx 50''$ SE of the PSC galaxy position (within the PSC error box). Unfortunately, this is only ~ 2.5 from the X-ray centroid of the quasar, and both the galaxy (if a genuine detection) and the quasar have very soft X-ray spectra. This means that the wings of the point spread function (PSF) for the quasar may contaminate the counts at the position of the galaxy.

To assess the possible effects of the quasar in creating a spurious X-ray source at the location of IRAS 14070, we have performed Monte Carlo calculations that mimic the detection algorithms performed on the actual X-ray data. We assume a PSF for the quasar which has a Gaussian core and $1/r^2$ wings. Because the PSF is energy dependent, a major limitation of our simulations is the uncertainty in the X-ray energy distribution of the quasar; we have assumed a power law with X-ray spectral slope $\alpha_x \approx -0.5$. In the simulations, we assume that there is no X-ray source at the position of IRAS 14070 and then look for the occurrence of sources arising spuriously from Poisson fluctuations in the wings of the synthetic "quasar." From over 1000 such Monte Carlo simulations, we expect a spurious source of the observed strength (or greater) falling within the error box ($90''$) of the IRAS galaxy position 0.54% of the time

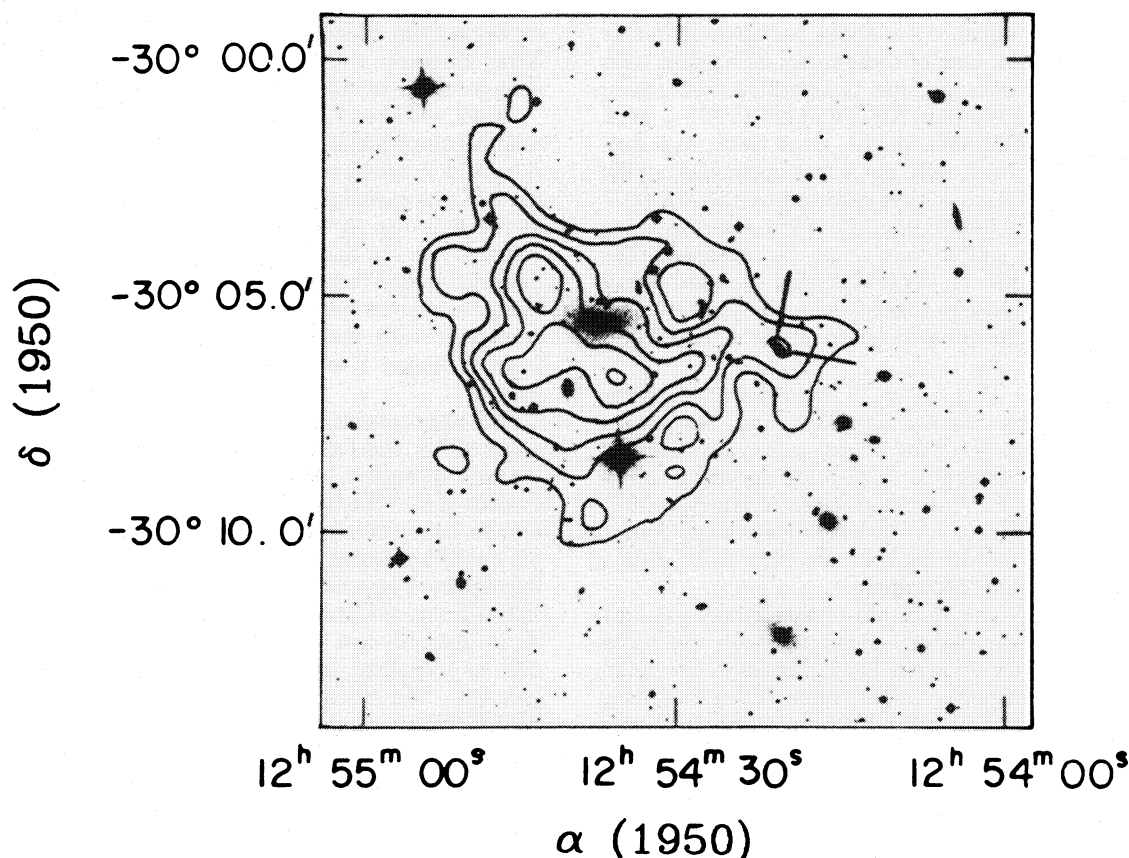


FIG. 2.—An enlargement of the red ESO survey print with contours of equal intensity X-ray emission from the vicinity of the cluster Klemola 22. Each contour is a factor of ~ 1.3 times fainter than the previous one; the peak intensity contour is $\approx 10^{-13}$ ergs cm^{-2} s^{-1} arcmin^{-2} . Bars indicate the position of IRAS 12543–3006, which may be a weak unresolved X-ray source.

or less. These simulations suggest that the “source” in the real data is unlikely to be spurious. If the measured X-ray flux is approximately correct, then the galaxy, an association of H II regions, is much brighter in X-rays than other galaxies of this type. Because of the uncertainties, we quote the X-ray flux as an upper limit in Table 1. This region merits further X-ray study, at higher spatial resolution.

IRAS 23461 is located next to a bright star which is detected by the automated algorithms. Thus, the X-ray data we list for this galaxy is a very conservative upper limit, since it probably includes considerable flux from the nearby star.

V. DISCUSSION

Our investigation of IRAS “warm” galaxies has revealed the X-ray detection of a small yet diverse group of AGNs. They include a cluster Seyfert 1 galaxy (IRAS 04124), a narrow-line Seyfert 1 galaxy (IRAS 04596), a Seyfert 1.9 galaxy (IRAS 14434), a Seyfert 2 galaxy (IRAS 12232), and a starburst galaxy (IRAS 02071). In addition, we detect extended X-ray emission from a cluster of galaxies that in projection includes a “warm” IRAS galaxy with strong emission lines. It is unclear whether this galaxy is itself detected in X-rays, and whether it is a true member of the cluster or a foreground galaxy; we exclude it from the discussion below.

The sample, both X-ray detections and upper limits, comprises 16 galaxies. There are three Seyfert galaxies with observed broad lines. One of these has both broad and narrow components to the Balmer lines. One has a low velocity width

of the permitted lines relative to the majority of Seyfert 1 galaxies, and the other is of Seyfert type 1.9, with no observable wings to the H β line profile. There are six Seyfert 2 galaxies. The rest fall into the rather heterogeneous classifications of starburst and H II region type, which for convenience we shall refer to as emission-line galaxies. We detect in X-rays all three of the Seyferts with observable BLRs, one Seyfert 2 galaxy, and one emission-line galaxy. The X-ray luminosities of the two Seyfert 1 galaxies are typical for that class, but the Seyfert 1.9 galaxy is underluminous in X-rays by comparison. This may be the result of low-energy X-ray absorption by a high column density, as inferred from the steep broad-line Balmer decrement. The Seyfert 2 NGC 4388 is somewhat underluminous in X-rays (Kriss, Canizares, and Ricker 1980), especially if the fainter broad wings reported by Filipenko and Sargent (1985) imply the presence of a Seyfert 1 component. On the other hand, the emission-line galaxy Mrk 1022 (NGC 838) has a high X-ray luminosity for its class. It is several times more luminous than NGC 7714 (Weedman *et al.* 1981). We note that the intrinsic X-ray luminosity may be higher still, since the Balmer decrement implies an $A_v \approx 2.5$, which suggests an N_H column higher than the line-of-sight Galactic column used to obtain the X-ray luminosity in Table 2.

Lower limits to the ratios of $(H\alpha + [N II])/X\text{-rays}$ for the other undetected emission-line galaxies are all consistent with the observed ratio in Mrk 1022, except in one case. For IRAS 00344 (ESO 350–IG38), this ratio is more than 2.7 times higher than in Mrk 1022. The optical spectrum of IRAS 00344 shows

a very blue continuum with high excitation lines of large velocity width. This may be related to its disturbed optical morphology. It has the highest 25 μm luminosity of the emission-line galaxies, and a higher $\text{H}\alpha$ luminosity than any of the 102 starburst galaxies studied by Balzano (1983). This information, together with the lack of any detectable late-type stellar absorption features, suggests that it is undergoing a very energetic burst of star formation. Although not detected in X-rays, this galaxy is clearly worthy of further study. It also demonstrates that the $\text{H}\alpha$ flux alone may not be a good indicator of X-ray flux for a heterogeneous sample of emission-line galaxies. Other parameters such as the mass function, metallicity and age of the starburst all play significant roles in determining the associated X-ray emission.

Taking as one group the Seyferts of all types, we detect 44% of our observed sample. However, we detect only one (14%) of the non-Seyfert emission-line galaxies. This is consistent with the fact that Seyfert galaxies have much higher X-ray luminosities than emission line galaxies. Two-sample nonparametric survival analysis yields $\langle \log L_x \rangle = 41.6 \pm 0.5$ and 40.6 ± 0.3 , respectively, for the two groups, at a significance level of 5% (i.e., 2σ). We find a detection rate of 32% for the entire sample. These percentages only have meaning in the context of the X-ray sensitivity of each observation. Although the exposure times differ, the sensitivities (0.5–3.0 keV) range from $1-3 \times 10^{-13} \text{ ergs cm}^{-2} \text{ s}^{-1}$ for a 2.6σ upper limit.

There was no *a priori* X-ray or optical selection criteria applied to these "warm" *IRAS* galaxies serendipitously observed by *Einstein*. The only exception is the inclusion of published optical data for *IRAS* 02071, for which we did not obtain optical spectroscopy. The inclusion of this galaxy may introduce a selection bias with the effect that the detection rate for non-Seyfert galaxies quoted above would be an upper limit.

Because of the small sample size, the X-ray detection percentages should be viewed as indicative. With these qualifications in mind, the percentages may be applied to the much larger complete sample of "warm" *IRAS*-selected galaxies (De Grijp, Miley, and Lub 1987), if they were to be observed with the same distribution of X-ray sensitivities. It is therefore likely that a large number of previously unknown Seyfert 1–1.9 galaxies selected by means of their warm *IRAS* colors could be detected in soft X-rays in future surveys by, for example, *ROSAT*.

We thank Dan Harris for his patient help interpreting X-ray confused regions. Mike Bolte and Ron Downes supplied additional optical spectra, helping to weed out galactic objects. Eric Feigelson and Takashi Isobe provided code for survival analysis. This work was supported by NASA grant NAG8-590.

REFERENCES

- Allen, C. W. 1973, *Astrophysical Quantities* (3d ed.; London: Athlone).
 Anderson, S. F., and Margon, B. 1987, *Ap. J.*, **314**, 111.
 Balzano, V. A. 1983, *Ap. J.*, **268**, 602.
 De Grijp, M. H. K., Miley, G. K., and Lub, J. 1987, *Astr. Ap. Suppl.*, **70**, 95.
 De Grijp, M. H. K., Miley, G. K., Lub, J., and de Jong, T. 1985, *Nature*, **314**, 240.
 ———. 1989, in preparation.
 Fabbiano, G., Feigelson, E., and Zamorani, G. 1982, *Ap. J.*, **256**, 397.
 Filippenko, A. V., and Sargent, W. L. W. 1985, *Ap. J. Suppl.*, **57**, 503.
 Harnden, F. R., Jr., et al. 1984, *Scientific Specification of the Data Analysis System for the Einstein Observatory (HEAO 2) Imaging Proportional Counter (SAO Special Rept., No. 393)*.
 Heckman, T. M. 1980, *Astr. Ap.*, **87**, 152.
 Heiles, C. 1975, *Astr. Ap. Suppl.*, **20**, 37.
IRAS Point Source Catalog. 1985, Joint *IRAS* Science Working Group (Washington, DC: US GPO) (PSC).
 Kailey, W. F., and Lebofsky, M. J. 1988, *Ap. J.*, **326**, 653.
 Keel, W. C., Kennicutt, R. C., Jr., Hummel, E., and van der Hulst, J. M. 1985, *A.J.*, **90**, 708.
 Kriss, G. A., Canizares, C. R., and Ricker, G. R. 1980, *Ap. J.*, **242**, 492.
 Marshall, F. J., and Clark, G. W. 1984, *Ap. J.*, **287**, 633.
 Neugebauer, G., et al. 1984, *Ap. J. (Letters)*, **278**, L1.
 Osterbrock, D. E., and Pogge, R. 1985, *Ap. J.*, **297**, 166.
 Petre, R., Mushotzky, R. F., Krolik, J. H., and Holt, S. S. 1984, *Ap. J.*, **280**, 499.
 Phillips, M. M., and Malin, D. F. 1982, *M.N.R.A.S.*, **199**, 905.
 Rowan-Robinson, M. 1985, *The Cosmological Distance Ladder* (New York: Freeman).
 Soifer, B. T., et al. 1984, *Ap. J. (Letters)*, **278**, L71.
 Stauffer, J. R. 1982, *Ap. J.*, **262**, 66.
 Steiner, J., Grindlay, J., and Maccacaro, T. 1982, *Ap. J.*, **259**, 482.
 Tananbaum, H., et al. 1979, *Ap. J. (Letters)*, **234**, L9.
 Tananbaum, H., Wardle, J. F. C., Zamorani, G., and Avni, Y. 1983, *Ap. J.*, **268**, 60.
 Ward, M. J., Done, C., Fabian, A. C., Tennant, A. F., and Shafer, R. A. 1988, *Ap. J.*, **324**, 767.
 Weedman, D. W., Feldman, F. R., Balzano, V. A., Ramsay, L. W., Sramek, R. A., and Wu, C.-C. 1981, *Ap. J.*, **248**, 105.
 Wood, K. S., et al. 1984, *Ap. J. Suppl.*, **56**, 507.
 Young, E., et al. 1984, *Ap. J. (Letters)*, **278**, L75.
 Zwicky, F., et al. 1961, *Catalogue of Galaxies and Clusters of Galaxies*, (Pasadena: California Institute of Technology).

S. F. ANDERSON: Mount Wilson and Las Campanas Observatories, 813 Santa Barbara Street, Pasadena, CA 91101-1292

M. H. K. DE GRIJP: Sterrewacht Leiden, Postbus 9513, 2300 RA Leiden, The Netherlands

P. J. GREEN: Department of Physics, FM-15, University of Washington, Seattle, WA 98195

B. MARGON: Department of Astronomy, FM-20, University of Washington, Seattle, WA 98195

G. K. MILEY: Space Telescope Science Institute, 3700 San Martin Drive, Baltimore, MD 21218

M. WARD: Institute of Astronomy, Madingley Road, Cambridge CB3 0HA, UK